RSC Advances

ROYAL SOCIETY OF CHEMISTRY

www.rsc.org/advances

Graphical Abstract

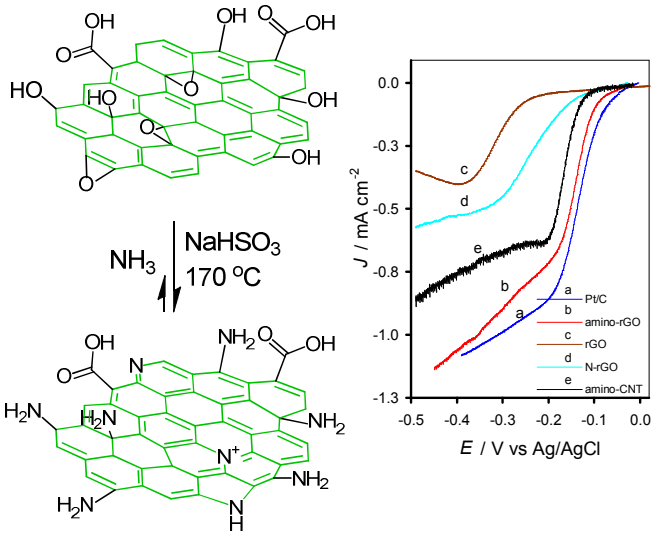

Efficient amine functionalization of graphene oxide through Bucherer reaction: An extraordinary metal-free electrocatalyst for oxygen reduction reaction

Aso Navaee [a] , Abdollah Salimi [a,b]*

[a] Department of Chemistry, University of Kurdistan, , 66177-15175, Sanandaj- Iran.

[b] Research Centre for Nanotechnology, University of Kurdistan, 66177-15175, Sanandaj- Iran.

*To whom correspondence should be addressed.

Tet:+9887333624001,Fax: :+9887333624008

E-mail: absalimi@uok.ac.ir, absalimi@yahoo.com (A. Salimi)

Abstract: A simple and reliable method based on the Bucherer reaction is proposed for the functionalization of graphene oxide (GO) with amine ($-NH_2$) groups. In the proposed method the chemical reaction between ammonia and GO ,as the precursor materials, is catalyzed with sodium bisulfite. The prepared amino-reduced graphene oxide (amino-r-GO) was characterized with spectroscopic and imaging techniques including FT-IR, XRD, XPS, SEM, EDX elemental mapping and thermal-gravimetric analysis (TGA). The surface analysis and material characterization reveal the high percentage of amine functional groups can be achieved via this method. The investigation of electrocatalytic activity of the prepared amino/r-GO toward oxygen reduction reaction confirms the significant improving the catalytic activity of amine functionalized graphene surface in the vicinity of doped nitrogen in same graphene framework. The onset potential of ORR vs. Ag/AgCl in 0.1 M KOH solution is observed at -0.05 V and peak current density is 1.15 mA cm^{-2} comparable to observed values for Pt/C as electrocatalyst (onset potential -0.04 and peak current density 1.17 mA cm^{-2}) . This prepared amino/r-GO is so important to future research for the extension of various graphene-based composites.

1. Introduction

The reaction of aromatic phenols such as naphthol with ammonia in the presence of sodium bisulfite to give naphthylamine was described in 1904 by Hans Th. Bucherer.[1] Afterward, this reaction was extensively used for other similar reactions.[2,3] We extended this reaction for the selective synthesis of amino-graphene. Graphene (Gr) as a two dimensional structure of sp^2 hybridized carbon, displays a variety of outstanding properties including high electron mobility at room temperature, exceptional thermal conductivity and remarkable mechanical properties.[4] Particularly, taking advantage of the electronic properties of this material has attracted a lot of researches. However, many of these interesting and unique properties can be improved via chemical functionalization of the surface or edge defects. These preliminary modifications enable chemical covalent bonding between the Gr and organic materials of interest and also, make Gr as an ideal platform to anchor various metal nanoparticles. Functionalized Gr is also usually easier to be dispersed in organic solvents and water, which can helps the functionalization of Gr by a number of functional groups.[5] In this context, chemical functionalized Gr which protected polymer composites, energy-related materials, sensors, field-effect transistors, photo-devices, adsorption, separation, chemical synthesizes and biomedical systems, have been widely reviewed.[6-11]

Graphene oxide (GO), having several kinds of oxygen functional groups,[6] has been directly used as a platform for adsorption of metal ions in aqueous solutions,[12] solid-phase extraction,[13,14] catalyst for many reactions[15] and preparation of various Gr-based composites.[16,17] However, nitrogen atom in amine is more nucleophilic than the oxygen atom. So, it is expected that the substitution of Gr or GO with amine increases the nucleophilic properties of Gr and as a consequence, interfacial binding between Gr and the materials of interest. Such interactions

improve performance and functionality of the intended applications of Gr. For example, the amine functionalization in carbon nanotube has been used to enhance the controlled covalent bonding to polymers or biological molecules.[18] More recently, different substituted amines have been embedded to GO to be applied in energy storage,[19] electrocatalytic oxygen reduction reactions (ORR)[20,21] electrochemical sensors,[22] solid basic catalyst in organic chemistry[23,24] and optical Gr quantum dots.[25,26] These wide potential applications of amino-Gr need a facile and controllable method to implant a high fraction of amine functional groups in Gr sheets.

Here, using the Bucherer reaction, GO is functionalized with amine ($-NH_2$) groups. The produced amino/r-GO is characterized by SEM (scanning electron microscopy), EDX (energy-dispersive x-ray spectroscopy), FTIR, XPS (x-ray photoelectron spectroscopy), XRD (X-ray diffraction) and TGA (thermal-gravimetric analysis). Compared to the previously reported results, this method gives a higher ratio of amine groups in the r-GO framework. As an example of its applications, the prospective catalytic of obtained amino/r-GO toward ORR is described. We believe that this amino/r-GO will be very important in future research for the extension of various graphene-based composites.

2. Experimental Section

2.1. Materials

The graphite powder, potassium permanganate, sodium nitrate, sulfuric acid, hydrogen peroxide, sodium bisulfite, ammonium hydrate, phosphate buffer salts, potassium hydroxide, hydrazine monohydrate (85%) and commercial platinum on activated carbon with 10% of Pt loading (Pt/C 10%) were purchased from Merck. NH_2 functionalized Multi-Walled Carbon Nanotubes (NH_2-MWCNTs),($-NH_2$ functionalization is aprox. 0.5%, measured by XPS)with

purity of 95%, surface specific area of 480 m^2 g^{-1}, diameter of 20-30 nm and 1 μM length were obtained from Drop Sens (Spain).

2.2. Instruments

The XRD analysis of the samples was performed with a Bruker D8 Advance powder diffractometer using Ni filtered CuKa radiation (k = 1.54056 Å). The XPS spectra of the supported catalysts were recorded on a VG Microtech Twin anode XR3E2 X-ray source and a concentric hemispherical analyzer operated at a base pressure of 5 $\times 10^{-10}$ mbar using AlKa (hm = 1486.6 eV). Peak fitting of all spectra were performed using the Shirley background correction and Gaussian–Lorentzian peak shapes. Binding energies (BEs) were referenced to C 1s peak at 284.5 eV. Low-resolution survey spectra, as well as higher-resolution spectra for C and N were collected. The FTIR spectra of KBr discs containing 0.1 mg of prepared amino-Gr well as chemically synthesized GO powders were obtained by a Vector-22 BRUKER spectrophotometer (Switzerland). Scanning electron microscopy (SEM) images and corresponding map and elemental analysis were obtained with a MIRA3 TESCAN HV: 20.0 KV from Czech Republic. Zeta potentials were obtained by a zeta potential analyzer form Malvern instrument Ltd. The electrochemical studies including cyclic voltammetry, linear sweep voltammetry and choronoamperometry were carried out using a μAUTOLAB modular electrochemical system (ECO Chemie, Ultrecht, The Netherlands) equipped with a PGSTAT 101 module driven by GPES software (ECO Chemie) in conjunction with a conventional three-electrode system (an Ag/AgCl / 3 M KCl and platinum wire as reference and counter electrode, respectively) and a personal computer for data acquisition and processing. For modification of glassy carbon (GC) electrode with each of nanomaterial, 5 μL of dispersed solution of these materials (5 $mgml^{-1}$ in ethanol) was cast on the electrode surface and dried at room temperature. To achieve nitrogen

and oxygen saturated solution before each experiment, the electrolyte solution was purged by nitrogen or oxygen gas for 5 min. Scan rates for recorded cyclic voltammograms was 0.01 Vs^{-1} and all experiments were done at room temperature (~298 K).

2.3. Preparation of amino-rGO

GO was synthesized according to modified Hummers method as described in the supporting information. The amination of GO was performed in an autoclave tube. In a typical synthesis, 50 mg of GO was well dispersed in 70 mL water. After that, 50 mmol NH_3 and 10 mmol sodium bisulfite ($NaHSO_3$) were added to the dispersed GO in an autoclave tube and it was kept in oven at ~170 °C for about 10 hours. After cooling to ambient temperature, the resulting material was washed via centrifugation and re-dispersion in fresh water 3 times to remove $NaHSO_3$ catalyst and non-reacted ammonium. The prepared amino-rGO is dried at vacuum and can be redisposed in water as well as organic solvents such as ethanol and dimethylformamide for desired applications

2.4.Preparation of graphene

We synthesized Gr using modified hummers method[27] as described in our previous work.[28] In brief; 1 g graphite powder was added to a mixture of 3 g $NaNO_3$ and 70 ml of concentrated H_2SO_4 in an ice bath. Then, 3 g $KMnO_4$ was gradually added at 15 min under stirring. The mixture was stirred for 2 h at ambient temperature and then diluted with deionized (DI) water and stirred for 30 min. After that, 5% H_2O_2 was added into the solution until the color of the mixture changed to yellow, indicating that graphite is fully oxidized. The as-obtained graphite oxide slurry was re-dispersed in DI water and then exfoliated to generate graphene oxide nanosheets (GONSs) using a bath ultrasonic. The mixture was then, filtered and washed with

diluted HCl solution to remove metal ions. Finally, the product was washed with DI water to remove the acid. Afterwards, the graphene oxide nanosheets have been reduced by hydrazine. In a typical process, 50 mg of obtained solid product were dispersed in 20 ml of H_2O via ultrasonication. Then 100 mg of poly (sodium 4-styrenesulfonate) (PSS, $(C_8H_7NaOS)_n$, Mw = 70,000) and 2.5 ml hydrazine (NH_2NH_2) were added into the dispersed GONSs. After stirring for 30 min, the mixture was transferred to a Teflon lined autoclave and held in an oven at 110 °C for 1 h. During the hydrothermal reaction, the PSS tethered to the GONSs layers and GONSs were reduced by hydrazine to graphene-PSS (Gr-PSS). The product was centrifuged and then washed with DI water and ethanol to remove the unreacted PSS surfactant. The final Gr product was dried in a vacuum oven at 60 °C.

2.5. Preparation of nitrogen doped graphene (N-Gr)

The synthesis of N-Gr was done according to the previously reported method.[29] In brief; GO (70 mg) was dispersed in water (100 mL) for 1 hour to yield a dark brown suspension. The suspension was centrifuged (5 min; 1000 rpm), and the remaining GO in solution was taken from the stable suspension for subsequent synthesis. Ammonia solution was added into the above suspension until a pH of 10 was reached and then 1.0 mL of hydrazine monohydrate was added under constant stirring. The suspension was placed in a stainless steel autoclave with a Teflon liner, and a hydrothermal treatment was carried out at 100 °C for 3 h. Finally, the suspension was centrifuged (5 min; 1000 rpm) and the solid was washed with deionized water and dried at 40 °C for 24 h.

3. Results and Discussions

3.1. Characterization

The chemical synthesis reaction between ammonia and GO, as the precursor materials, is catalyzed with sodium bisulfite according to the following equation:

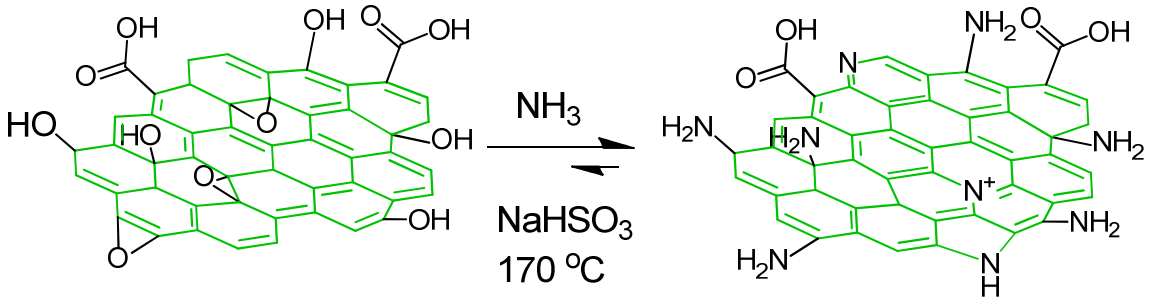

The reaction is completed in a typical autoclave tube over night at the temperature of ~170 °C. During the single displacement reaction in hydrothermal condition, phenolic oxygen located at the surface and the edge plane of GO, are replaced by -NH_2 groups resulting in amino-Gr. Moreover, during the hydrothermal condition the epoxy groups are removed and the GO platelets are reduced to r-GO nanosheets.

It is well known that Bucherer reaction is the reversible conversion of naphthol to naphthyl amine. In the case of GO functionalization process, the initial reactants have a high dispersibility or frequently, solubility in aqueous solution while, after amine functionalization the resultant product (amino-rGO) is almost insoluble, even its dispersibility in water is drastically decreased compare to GO. Therefore, we believe the amination process of GO through bucherer reaction is mostly proceed in the forward direction, so this process has a little reversibility.

As discussed above, GO has a higher dispersibility rather than amines functionalized GO in water. Moreover, the single sheets of GO are dissolved in water after dispersion and the color of solution changed to yellow. Hence, the exfoliated GO might be better for functionalization but

various chemical reactions or physical interaction need to other functional groups beyond the oxygen functional groups. The stability of amino-rGO is higher than GO and rGO on the electrode surface, indicating the high affinity of amino groups for electrostatic or other possible interactions with other vicinal materials.

In contrast to GO, amino-rGO is more dispersible in water and also provides higher conductivity. The stability of colloidal dispersions can evaluated by measurement of Zeta potential.[30] For solvent containing of dispersed GO or amino-rGO the magnitude of the Zeta potential designates the degree of electrostatic repulsion between similarly charged surfaces of vicinal sheets. Table 1 compares the Zeta potentials and also conductivity of water-dispersed GO and amino-rGO. The amount of Zeta potential for amino-rGO was obtained to be -29.7 which about 9.8 point higher than that for GO, indicating the greater stability of colloidal dispersion amino-rGO. Moreover, the conductivity of amino-rGO dispersed solution is ~2.2 fold greater rather than GO under such condition. This confirms the fact that amination process improve the conductivity of GO compared to chemical reduction.

Here Table 1

The SEM images of GO and amino-rGO are shown in Figure 1A and 1B, respectively. The GO morphology resembles a thin curtain in Figure 1A and some single flakes with relatively large surfaces can be seen, indicating the respectable exfoliation of graphite during oxidation process. Whiles, the amino-rGO sheets are informally folded on each other with many ripples and seem to form the tangled patches. Between the crosswise edges of the multi-layer of amino-rGO a porous network with a size ranging from 100 to 500 nm, is clearly observable. These specifications could be related to the hydrogen bending of amino surface functional groups. The

EDX elemental mapping (Figure 1D,E) of carbon and nitrogen of a large area of amino-Gr dispersed powder (Figure 1C) illustrate a homogeneous distribution of N functionalities on the graphene structure. The EDX elemental analysis, which is given in Table 2, reveals 62.85, 12.22, 24.92 weight% (W%) and 68.28, 11.39, 20.33 atomic% (A%) for C, N and O, respectively. Based on our best knowledge, such highly N content in graphene structure has not been reported before.

In order to investigate the phase and structure, GO and amino-rGO were also characterized by powder XRD (Figure 1F). The strong diffraction peak of GO is located at a 2θ=10.7°, indicating the layer-to-layer distance of 0.83 nm based on the Bragg equation, owing to the introduction of various oxygen-containing groups and water molecules. Whereas, the diffraction peak of the amino-Gr moves to a lower 2θ angle with a d-spacing of 1.10 nm, which is 0.27 nm larger than that of GO, and 0.77 nm larger than the lattice spacing of graphite (d-spacing=0.334 nm). The increase in the layer-to-layer distance signifies the fact that $–NH_2$ groups, covalently attached to the GO surface and many of layers are well separated, which it is more appropriate for the embedding the desired materials. The broad diffraction peak at around 2θ=~26° with d-spacing of 0.342 nm is attributed to the disordered stacking structures of amino-Gr layers.[22,25]

Here Figure 1

Here Table 2

The comparison of FTIR spectra (Figure 2A) of GO before (a) and after (b) chemical amination implies some changes in the chemical nature of GO during the amination process. GO displays a broad FTIR peak at 3500-2500 cm^{-1} attributed to the stretching of adsorbed water molecules and structural O–H groups (such as alcohol and carboxylic acid) which do not allow distinction

between C–OH and H_2O peaks.[27] The sharp peak at 1715 cm^{-1} is attributed to the C=O stretching of carboxylic acid group, 1614 cm^{-1} to the sp^2 C=C and conjugated C=O stretching, 1213 cm^{-1} and 1040 cm^{-1} to C–O stretching of phenolic and epoxy groups, respectively.[31] In the case of amino-rGO, two almost distinct sharp peaks at 3409 and 3424 cm^{-1} attributed to N-H stretching, which overlapped with a broad peak arisen from carboxylic acid stretching, can be seen. Moreover, compared to GO, the bandwidth at 3500-2500 cm^{-1} and the intensity of all peaks attributed to oxygen functional groups are remarkably decreased, indicating that most of GO oxygen species are reduced or substituted with amino groups during the ammination process. Other outstanding differences are observed in the appearance of the two peaks at 1550 and 1150 cm^{-1} attributed to N-H bending and C-N stretching. Hence, FTIR analysis confirms the amine functionalization of GO followed by reduction to amino-rGO.

The chemical nature of the resulted material was evaluated by XPS analysis. The survey spectra of obtained amino-rGO as well as Gr (chemically reduced GO) are given in the Figure 2B and the high resolution scan spectra of C1s and N1s are shown in Figure 2C and D. Unlike GO, besides the carbon and oxygen, nitrogen appears in the survey spectra of amino-rGO (Figure 2B). Based on the XPS data and according to the atomic sensitivity factors, the relative abundance of C, N and O elements on the surface of the sample was calculated to be 68.7, 8.1 and 23.2 atomic%, respectively. These results are in good agreement with the EDX analysis. Peak fitting of C1s and N1s high resolution spectrum reveals the various carbon and nitrogen components in the amino-rGO framework. The percentages of these species are given in Table 2. As shown in Figure 2C, carbon atom exists in different functional groups: C–C/C=C (284.6 eV), C–N/C=N (285.8 eV), C-O (286.7 eV), C=O (287.9 eV), and COOH (289.4 eV). In the case of nitrogen atom, the amination process lead to the formation of N=C (398.4 eV), C-NH_2 (399.4

eV), C-N-C (400.8 eV), C-N^+-C or graphitic nitrogen (402.1 eV) and N-oxide (403.2 eV).[19-26] As can be seen in Figure 2D, the most intense peak assigned to the C-NH_2, indicating that amino functionalized rGO can be made almost selectively via the suggested method. It is expected that the amino functional groups in the vicinity of doped nitrogen can improve the catalytic property of rGO.

Here Figure 2

Here Table 2

To gain additional insight about the fraction of functional groups on GO, reduced GO (rGO) and amino-rGO, TGA was performed under a nitrogen atmosphere in a temperature range of 34–800 °C with a ramp rate of 15 °C min^{-1} (Figure 3). For GO there are three stages of weight loss. The first stage with a rapid weight loss occurs at about 168 °C which is just about 16.5 W% of the total mass remains, mostly attributed to the removal of the trapped water molecules and epoxy oxygen functional groups. The second stage occurs at 470 °C with 8 W% of total remaining weight and can be attributed to the removal of phenolic groups and decomposition of sp^3 hybridized carbon atoms located at the defect site of GO. This result indicates the high degree of oxidation of graphite after chemical exfoliation. However, for rGO, there is almost no weight loss below 525 °C and even after that, 78 W% of the mass remains, demonstrating the effective reduction and removal of oxygen functional groups. Comparing to GO, after amine functionalization, the thermal stability increases and a large mass loss (88 W%) appears at about 588 °C. This can be attributed to the decomposition of amino-carbons, which is similar to the previously reported results for amine grafted rGO.[24] So, the larger thermal stability compared to

GO and the larger mass losing compared to rGO indicate the efficient displacement of oxygen moieties by amino groups during the chemical ammination of GO.

Here Figure 3

3.2. Electrocatalytic behavior of the resulted amino-graphene

High electrocatalytic activity towards ORR is important for potential fuel cell catalysts. Metal-free carbon-based ORR electrocatalysts have recently been validated as promising low-cost alternatives to platinum-based catalysis due to their wide availability, high stability, unique surface properties and environmental acceptability.[32-35] The ORR catalytic performance of amino-Gr was first investigated by cyclic voltammetry (CV) and comparative studies were performed by linear sweep voltammetry (LSV). As illustrated in Figure 4A, a well-defined cathodic peak under O_2-saturation condition in 0.1 M KOH is clearly observed, when the onset ORR potential located at -0.07 and the plateau region reaches to -0.19 V vs Ag/AgCl. These ORR onset or peak potential is more positive than that of other recently reported metal-free ORR catalysts such as N-graphene,[32] co-doped graphene,[33] and amine functionalized GO,[20,21] indicating that the high catalytic activity of Gr can be obtained via amine functionalization. Also, the continuous chronoamperogram was recorded at the potential value of -0.2 V to investigate the long-term activities of amino-rGO. As shown in the inset of Figure 3A, after about 4 hours no significant decreases are observed.

To compare the electrocatalytic activity, similar LSV curves were obtained for commercial platinum on activated carbon (Pt/C 10%), Gr, N-Gr and commercial amino-CNT as well as for the as-obtained amino-rGO (Figure 3B). The limiting current density of ORR on the obtained

amino-rGO is comparable to Pt/C but it is significantly higher than that of the other mentioned catalysts. Remarkably, the onset potential of ORR (-0.07 V) is close to that of commercial Pt/C (-0.04 V) and much more positive than that of Gr (-0.24 V), N-Gr (-0.14 V) and commercial amino-CNT (-0.12). The higher limiting current density and a smaller amount of ORR overpotential on amino-rGO obviously demonstrate the high catalytic performance of this material. Also, it can be a good candidate as the supporting material for metal nanoparticles to attain different solid basic catalysts with higher catalytic performance.

Here Figure 4

4. Conclusion

In summary, we have proposed the Bucherer reaction as an effective, facile, selective and reliable method to synthesis of amine functionalized grapheme oxide. The product analysis showed, the high percentage of amine groups covalently attach to the graphene oxide and the functionalized grapheme oxide sheets with amine have a larger layer-to-layer distance. Even though the as-synthesized amino-rGO displays superior electrocatalytic activity and stability towards ORR. This detachment with the support of cover amine groups can assist the immobilization of biomolecules and organic materials or high loading metals nanoparticles to obtain graphene-based composite materials for development of high performance and flexible electrocatalyst for fuel cells and bioelectronic devices.

Acknowledgments: This research was supported by the Iranian Nanotechnology Initiative and the Research Office of the University of Kurdistan. We thanks Miss Masomeh Kurd(Zanjan Medical University) for measuring of samples Zeta potentials .

References

1 H.T. Bucherer, *J. Prakt. Chem*., 1904, **69**, 49–91.

2 H. Seeboth. *Angew. Chem. Int. Ed*., 1967, **6**, 307-317.

3 M.B. Smith, J. March. *March's Advanced Organic Chemistry*. John Willy and Sons Ltd. **2001**.

4 D. Jiang, Z. Chen (Eds), *Graphene Chemistry: Theoretical Perspectives*. John Willy and Sons Ltd. **2013**.

5 D. Wu, F. Zhang, P. Liu and X. Feng, *Chem. Eur. J*., 2011, **17**, 10804-10812.

6 D.R. Dreyer, S. Park, C.W. Bielawski and R.S. Ruoff, *Chem. Soc. Rev*., 2010, **39**, 228–240.

7 V. Singh, D. Joung, L. Zhai, S. Das, S.I. Khondaker and S. Seal, *Prog. Mater. Sci*., 2011, **56**, 1178–1271.

8 V. Georgakilas, M. Otyepka, A.B. Bourlinos, V. Chandra, N. Kim, K.C. Kemp, P. Hobza, R. Zboril and K.S. Kim, *Chem. Rev*., 2012, **112**, 6156–6214.

9 A. Schlierf, P. Samori and V. Palermo, *J. Mater. Chem. C,* 2014, **2**, 3129-3143.

10 M. Bacon, S.J. Bradley, T. Nann, *Part. Part. Syst. Charact*., 2014, **31**, 415–428.

11 S. Eigler and A. Hirsch, *Angew. Chem. Int. Ed.,* 2014, **53**, 2-21.

12 R. Sitko, E. Turek, B. Zawisza, E. Malicka, E. Talik, J. Heimann, A. Gagor, B. Feista and R. Wrzalik, *Dalton Trans*., 2013, **42**, 5682-5689.

13 Q. Liu, J. Shi, J. Sun, T. Wang, L. Zeng and G. Jiang, *Angew. Chem. Int. Ed*., 2011, **50**, 5913-5917.

14 R. Shi, L. Yan, T. Xu, D. Liu and Y. Zhu, *J. Chromatogr. A,* 2015, **1375**, 1-7.

15 J. Pyun, *Angew. Chem., Int. Ed*., 2011, **50**, 46–48.

16 A. Navaee, A. Salimi and F. Jafari, *Chem. Eur. J.,* 2015, **21**, 4949-4956.

17 A. Navaee, A. Salimi, *J. Mater. Chem. A,* 2015, **3**, 7623-7630.

18 T. Ramanathan, F.T. Fisher, R.S. Ruoff and L.C. Brinson. *Chem. Mater*., 2005, **17**, 1290-1295.

19 C.M. Chen, Q. Zhang, X.C. Zhao, B. Zhang, Q.Q. Kong, M.G. Yang, Q.H. Yang, M.Z. Wang, Y.G. Yang, R. Schlogl and D.S. Su*, J. Mater. Chem*., 2012, **22**, 14076–14084.

20 C. Zhang, R. Hao, H. Liao and Y. Hou, *Nano Energy,* 2013, **2**, 88–97.

21 Z. Jiang, Z. Jiang, X. Tiana and W. Chen, *J. Mater. Chem. A,* 2014, **2**, 441–450.

22 B. Wang, B. Luo, M. Liang, A. Wang, J. Wang, Y. Fang, Y. Chang and L. Zhi, *Nanoscale,* 2011, **3**, 5059–5066.

23 F. Zhang, H. Jiang, X. Li, X. Wu and H. Li, *ACS Catal*., 2014, **4**, 394−401.

24 C. Yuan, W. Chen and L. Yan, *J. Mater. Chem*., 2012, **22**, 7456–7460.

25 H. Tetsuka, R. Asahi, A. Nagoya, K. Okamoto, I. Tajima, R. Ohta and A. Okamoto, *Adv. Mater*., 2012, **24**, 5333–5338.

26 G.S. Kumar, R. Roy, D. Sen, U.K. Ghorai, R. Thapa, N. Mazumder, S. Saha and K.K. Chattopadhyay, *Nanoscale,* 2014, **6**, 3384–3391.

27 W.S. Hummers and R.E. Offeman, *J. Am. Chem. Soc.* 1958, **80**, 1339.

28 A. Navaee and A. Salimi, *Electrochim. Acta* 2013, 105, 230–238.

29 Q. He, Q. Li, S. Khene, X. Ren, F.E. Lopez-Suarez, D. Lozano-Castello, A. Bueno-Lopez and G. Wu, *J. Phys. Chem. C,* 2013, **117**, 8697−8707.

30 R.J. Hunter, Zeta potential in colloid science: principles and applications. London, UK: Academic Press; **1988**.

31 Spectral Database for Organic Compounds, SDBS, http://sdbs.db.aist.go.jp/sdbs/cgi-bin/cre_index.cgi

32 C. He, Z. Li, M. Cai, M. Cai, J.Q. Wang, Z. Tian, X. Zhang and P.K. Shen, *J. Mater. Chem. A*, 2013, **1**, 1401-1406.

33 J. Liang, Y. Jiao, M. Jaroniec and S.Z. Qiao, *Angew. Chem. Int. Ed*., 2012, **51**, 11496 – 11500.

34 Y. Zheng, Y. Jiao, M. Jaroniec, Y. Jin and S.Z. Qiao, *small,* 2012, **8**, 3550–3566.

35 N. Daems, X. Sheng, I. F. J. Vankelecom and P.P. Pescarmona, *J. Mater. Chem. A,* 2014, **2**, 4085–4110.

Figures captions

Table 1. Zeta potential values as well as conductivity of water-dispersed rGO and amino-rGO.

Table 2. EDX elemental analysis of amino-Gr.

Table 23: Approximate values of carbon and nitrogen containing functional groups in amino-Gr.

Figure 1. SEM images of GO (A) and amino-rGO synthesized by present method (B). C shows the SEM image of a large area of dispersed powder of amino-rGO on the Al wafer for elemental analysis. D and E represent the corresponding EDX elemental mapping of C and N of the area which shown in E, respectively. F represents the XRD patterns of GO and amino-rGO.

Figure 2. FTIR spectra of GO and amino-rGO (A). XPS survey spectra of Gr and and amino-rGO (B). High resolution XPS spectra of C1s (C) and N1s (D) of the prepared and amino-rGO.

Figure 3. TGA curves of GO, rGO (Gr) and amino-rGO.

Figure 4. A) CVs obtained by and amino-rGO modified glassy carbon electrode under N_2-saturated (upper) and O_2-saturated (bottom) solution in 0.1 M KOH. Inset of A represents the chronoamperometery curve obtained by amino-rGO modified electrode at O_2-saturated solution in 0.1 M KOH. B) LSV curves under O_2-saturated solution in 0.1 M KOH for many of electrocatalysts including Pt/C (a), and amino-rGO which obtained in this work (b), Gr (c), N-Gr (d) and commertial amino-CNT(e).

Table 2. Zeta potential values as well as conductivity of water-dispersed rGO and amino-rGO.

Sample	Zeta Potential (mV):	Zeta Deviation (mV):	Conductivity (mS cm^{-1})
rGO	-20.1	8.84	0.0293
amino-rGO	-29.7	10.5	0.0638

Table 2. EDX elemental analysis of amino-rGO

Elt	Line	Int.	Error	K	Kr	W%	A%	ZAF	Formula	Ox%	Pk/Bg	Class	LConf	HConf	Cat#
C	Ka	104.2	4.89	0.84	0.54	**62.85**	**68.28**	0.85		0.00	53.35	A	61.26	64.44	0.00
N	Ka	3.1	4.89	0.04	0.02	**12.22**	**11.39**	0.20		0.00	55.42	A	10.45	14.00	0.00
O	Ka	26.5	4.89	0.12	0.08	**24.92**	**20.33**	0.32		0.00	16.06	A	23.68	26.17	0.00
Total				1.00	0.64	100.00	100.00			0.00					0.00

Table 2: Approximate values of carbon and nitrogen containing functional groups in amino-rGO.

Carbon	**Species**	**C–C/C=C**	**C–N/C=N**	**C-O**	**C=O**	**COOH**
	Bending energy (eV)	284.6	285.8	286.7	287.9	289.4
	Percentage%	55.2	21.3	12.4	5.9	5.2
Nitrogen	Species	N=C	C-NH_2	C-N-C	C-N^+-C (graphitic type)	N-oxide
	Bending energy (eV)	398.4	399.4	400.8	402.1	403.2
	Percentage%	10.4	51.6	24.6	11.4	2.1

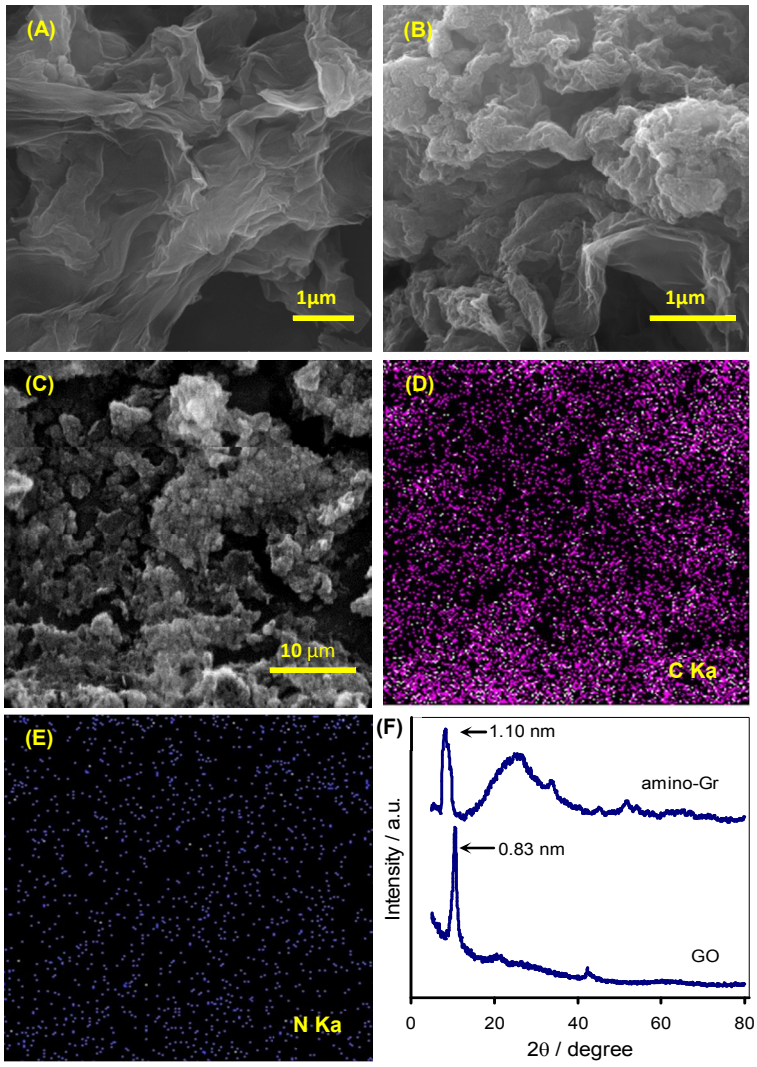

Figure 1

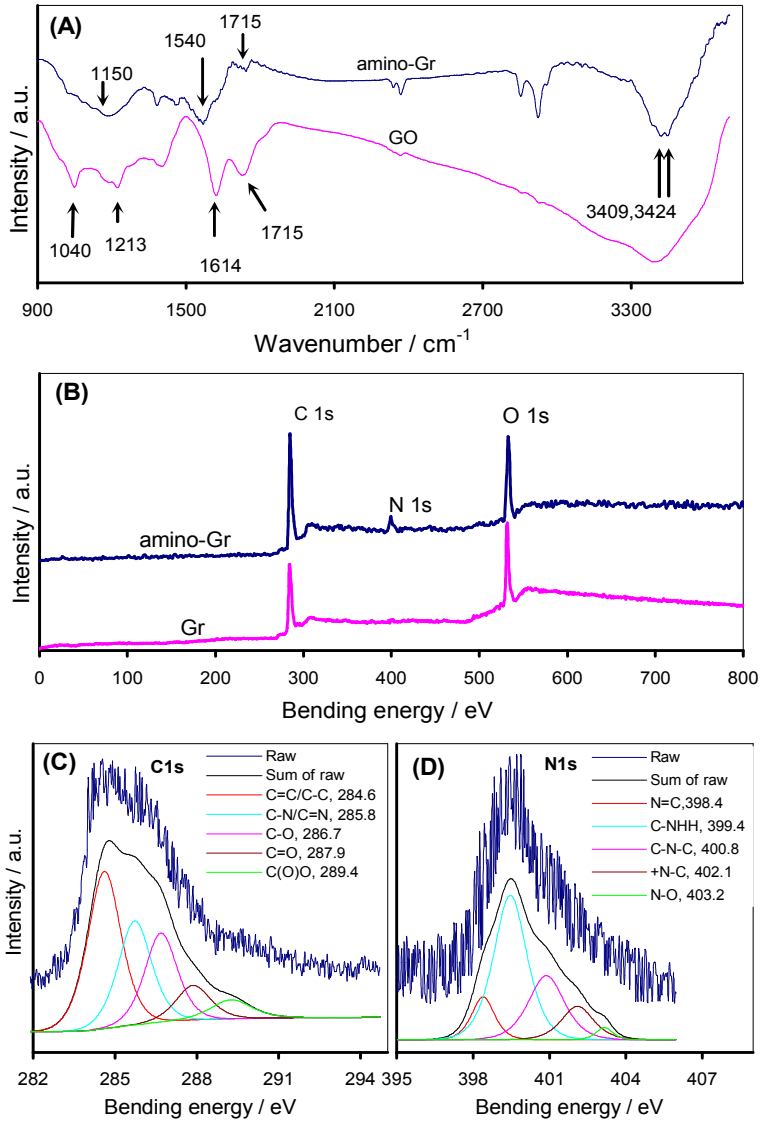

Figure 2

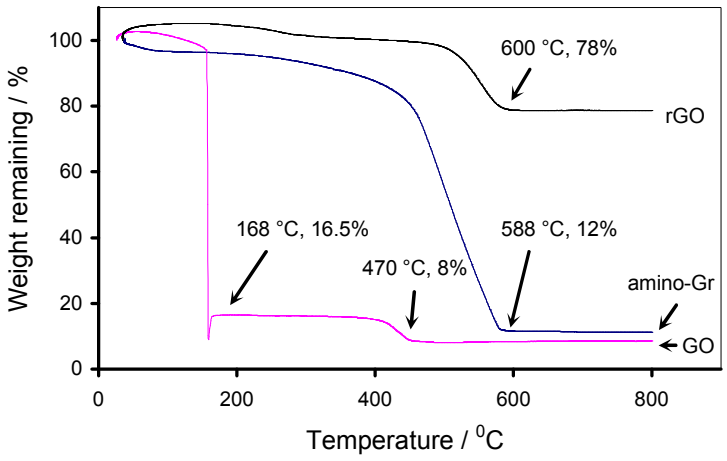

Figure 3

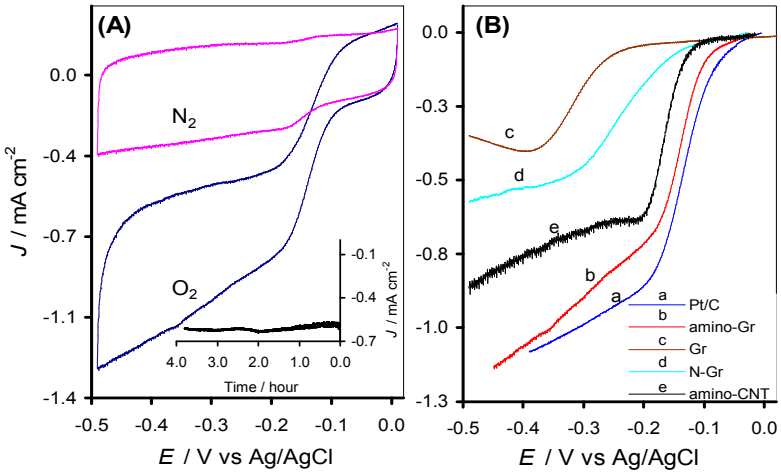

Figure 4

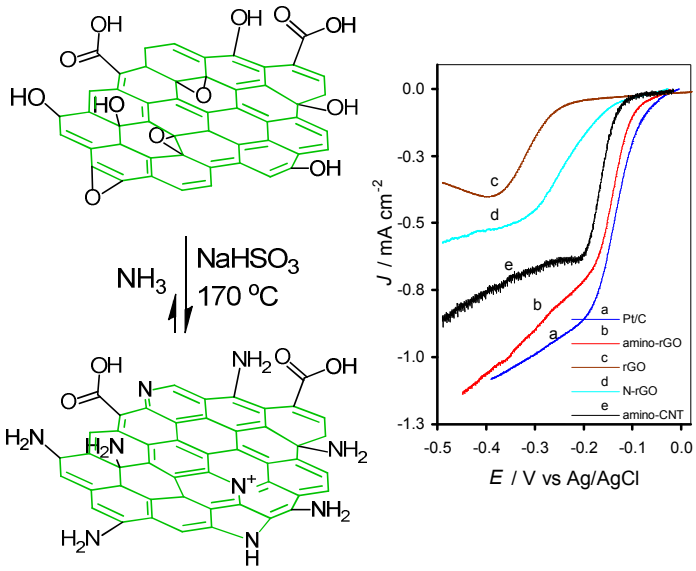

Graphical Absctract